

# Non-thermal emission from Pulsar-Wind Nebulae in Starburst Galaxies

S. Ohm,<sup>1,2</sup> and J.A. Hinton<sup>1</sup>

<sup>1</sup> *Department of Physics and Astronomy, The University of Leicester, University Road, Leicester, LE1 7RH, United Kingdom*

<sup>2</sup> *School of Physics & Astronomy, University of Leeds, Leeds LS2 9JT, UK*

Accepted 2012 October 31. Received 2012 October 23; in original form 2012 September 21

## ABSTRACT

The recently detected  $\gamma$ -ray emission from Starburst galaxies is most commonly considered to be diffuse emission arising from strong interactions of accelerated cosmic rays. Mannheim et al. (2012), however, have argued that a population of individual pulsar-wind nebulae (PWNe) could be responsible for the detected TeV emission. Here we show that the Starburst environment plays a critical role in the TeV emission from Starburst PWN, and perform the first detailed calculations for this scenario. Our approach is based on the measured star-formation rates in the Starburst nuclei of NGC 253 and M 82, assumed pulsar birth periods and a simple model for the injection of non-thermal particles. The two-zone model applied here takes into account the high far-infrared radiation field, and different densities and magnetic fields in the PWN and the Starburst regions, as well as particle escape. We confirm that PWN can make a significant contribution to the TeV fluxes, provided that the injection spectrum of particles is rather hard and that the average pulsar birth period is rather short ( $\sim 35$  ms). The PWN contribution should lead to a distinct spectral feature which can be probed by future instruments such as CTA.

**Key words:** radiation mechanisms: non-thermal – pulsars: general – galaxies: starburst

## 1 INTRODUCTION

Starburst (SB) galaxies have a very high star-formation rate (SFR) and hence supernova (SN) rate in a very localised region – the SB region – which is often located in the centre of the galaxy. The paradigm of cosmic-ray acceleration in supernova remnant shock fronts and the very large amounts of gas in the SB region, available for proton-proton interactions and subsequent  $\pi^0$ -decay  $\gamma$ -ray emission, made them suspected emitters of high-energy (HE;  $100 \text{ MeV} \leq E \leq 100 \text{ GeV}$ ) and very-high-energy (VHE;  $E \geq 100 \text{ GeV}$ )  $\gamma$ -rays (e.g. Völk et al. 1989; Akyuz et al. 1991) emission. Indeed,  $\gamma$ -ray emission from the prototypical SB galaxies NGC 253 and M 82 using the space-based Fermi-LAT (Abdo et al. 2010) and the ground-based Cherenkov telescopes H.E.S.S. and VERITAS (Acero et al. 2009; VERITAS Collaboration 2009) has recently been reported. There are no indications of  $\gamma$ -ray variability, and in the one case where the instrumental resolution is sufficient to discriminate, the TeV signal from NGC 253, the emission is compatible with originating in the SB nucleus, without a significant contribution from the disc of the galaxy (Abramowski et al. 2012).

Interpretations of the detected GeV and TeV  $\gamma$ -ray emission from SB galaxies are possible within the traditional framework if  $\sim 10\%$  of the kinetic energy of SN explosions is converted into particle acceleration and about (20 – 30)% of these protons lose their energy in interactions with target material (see e.g. Lacki

et al. 2011; Ohm & Hinton 2012; Paglione & Abrahams 2012; Abramowski et al. 2012). Whilst this scenario is certainly plausible, it may be somewhat oversimplified. For example, it is not clear that a contribution from individual sources can safely be neglected at all energies. The TeV  $\gamma$ -ray source population observed in our own Galaxy is diverse and shows emission from  $\gamma$ -ray binaries, stellar clusters, pulsar wind nebulae (PWNe), as well as SNR, with PWNe being the dominant object class (e.g. Hinton & Hofmann 2009). Based on this observation, Mannheim et al. (2012) argued that a major part of the emission seen in the TeV band from NGC 253 and M 82 could be explained by the combined emission from individual PWNe. The authors used the Galactic population of TeV-detected PWNe to estimate the contribution of leptonic  $\gamma$ -ray emission to the signal seen from both SB galaxies. However, the environment in which most of these PWNe evolve is significantly different from the physical conditions in SB nuclei. In this work we follow the idea of Mannheim et al. (2012), but study the PWN population and the resulting non-thermal emission in the SB based on the SFR and time-dependent pulsar injection power, rather than the (incomplete) sample of Galactic TeV PWNe.

## 2 PWN IN A STARBURST ENVIRONMENT

Pulsar wind nebulae are formed when the cold ultra-relativistic wind from a pulsar interacts with its environment. Particles in

PWNe are accelerated up to  $\sim 1$  PeV and produce synchrotron and Inverse Compton (IC) emission from radio to VHE  $\gamma$ -ray energies in interactions with magnetic and radiation fields, respectively (e.g. Gaensler & Slane 2006). The majority of PWNe in the Milky Way evolve in the Galactic disc, where the target radiation fields for the IC process are the Cosmic Microwave Background (CMB), visible starlight, and reprocessed starlight in the infrared. The typical energy densities of these radiation fields are  $U_{\text{ph}} \sim 1 \text{ eV cm}^{-3}$ . The dominant radiation field in the nuclear region of SB galaxies, on the other hand, is far-infrared (FIR) radiation with orders of magnitude higher energy density. Melo et al. (2002) for example found a total FIR luminosity of  $2 \times 10^{10} L_{\odot}$  in the SB region of NGC 253. The NGC 253 SB has a cylindrical shape with a radius of  $\sim 150$  pc and a half-height of  $\sim 60$  pc (Weaver et al. 2002). Assuming that each point in the cylinder radiates with the same emissivity at the temperature of the cold dust ( $\approx 50$  K),  $U_{\text{ph,NGC 253}} \simeq 2400 \text{ eV cm}^{-3}$ , a factor 2.9 higher than for a point source with the same luminosity at 150 pc distance<sup>1</sup>. This value is more than three orders of magnitude higher than is typical in the ISM and implies that the cooling time of highly-relativistic electrons in the SB region is much shorter, i.e.  $\sim 200$  yrs compared to  $\sim 3 \times 10^5$  yrs for a 1 TeV electron. IC cooling in such an environment will dominate over synchrotron losses unless  $B \gtrsim 500 \mu\text{G}$ .

The central source that powers the PWN is a pulsar that spins down and converts a fraction of its rotational energy into non-thermal particles and subsequently into radiation. Over time the pulsar's rotation slows down, and the energy put into the nebula decreases. The spin-down luminosity evolves in time as

$$\dot{E}(t) = \dot{E}_0 / (1 + t/\tau)^p, \quad \text{with } \tau = P_0 / \dot{P}_0 (n - 1), \quad (1)$$

where  $\tau$  is the characteristic spin-down time, given by the birth period of the pulsar  $P_0$  and the first derivative of  $P_0$ .  $p = (n + 1)/(n - 1)$ , where  $n$  is the braking index and is measured only for a handful of pulsars, where it lies between  $\sim 2$  and 3. In order to investigate the effect of the different radiation fields we will apply a single-zone, time-dependent model, where particles are injected according to Equation 1. This approach is similar to the one followed in Hinton & Aharonian (2007).

Figure 1 shows the fraction of the total injected electron power that is radiated in different spectral bands for a PWN evolving in both SB-like, and ISM-like environments for different ages. Particles are injected according to a power-law in energy  $N(E) \propto E^{-\alpha}$  with index  $\alpha = 2.0$ . Recent studies of prominent Galactic PWNe (Zhang et al. 2008, e.g.) suggest that the conversion efficiency of spin-down power into non-thermal particles  $\epsilon$  is  $\sim 1/3$ , with a recent lower limit of 0.3 derived for MSH 15–52 Schöck et al. (2010). However, the fraction of spin-down power that is converted into magnetic fields in young PWN is known to be small (Kennel & Coroniti 1984; Del Zanna et al. 2006; Gelfand et al. 2009; Tanaka & Takahara 2010, e.g.), so that  $\epsilon$  may approach 1. Non-radiative losses and/or complex spectral shapes for the lower energy particles may be responsible for the apparently lower injected power in particles (Spitkovsky 2008; Slane et al. 2010, e.g.). In the following we assume a constant value of  $\epsilon = 0.5$  and neglect non-radiative losses, with an estimated uncertainty of a factor of 2 in either direction.

Figure 1 illustrates that emission from an object evolving in a typical ISM region is likely to be synchrotron-dominated at early

times, when the  $B$ -field is high. At later stages, when the magnetic field decreases as the nebula expands, the fraction of energy converted into IC emission is expected to increase. This effect provides a plausible explanation for the number of bright, middle-aged PWNe detected in VHE  $\gamma$  rays that have rather low X-ray flux (see e.g. de Jager & Djannati-Ataï 2009). It has been suggested that such (more numerous) middle-age PWN may be the main contributors to the VHE emission of SB galaxies (Mannheim et al. 2012). However, the energy output of a Crab-like pulsar after  $10^3$  years is expected to be a factor of  $\sim 50$  higher than at an age of  $10^4$  years, more than compensating for the smaller number of young objects. In a typical ISM environment these younger objects would be expected to be synchrotron-dominated, with low IC efficiency. Due to the high energy density of radiation in a SB region, however, a large fraction of the non-thermal energy is expected to be emitted as IC radiation at GeV – TeV energies. Since the cooling time for the IC process is so short in this environment, electrons with an energy as low as  $\sim 20$  (200) GeV are efficiently cooled for a PWN age of  $10^4$  ( $10^3$ ) years (Figure 1, right).

### 3 EMISSION FROM THE PWN POPULATION

The results obtained in the previous section suggest that the recent particle injection history is of most importance when studying the HE and VHE  $\gamma$ -ray emission from a population of PWNe in SB galaxies. In the following we will investigate how a population of PWNe might evolve in an environment similar to the one found in the SB nuclei of NGC 253 and M 82. The most important pulsar-related properties that impact the overall level of non-thermal emission from PWNe in SB galaxies are (1) the number of pulsars that form PWNe, (2) the efficiency  $\epsilon$  with which these convert rotational spin-down energy to non-thermal particles, and (3) the distribution of pulsar birth periods, as these determine the time evolution of particle energy input.

#### 3.1 NGC 253

Based on the FIR luminosity in the SB nucleus of NGC 253, Melo et al. (2002) derive a SFR of  $\sim 3.5 M_{\odot} \text{ yr}^{-1}$ . With a Salpeter initial mass function and assuming that only stars with masses between  $8 M_{\odot}$  and  $20 M_{\odot}$  undergo type-II SN explosions and hence form pulsars, we estimate a type-II SN rate in the SB nucleus of NGC 253 of  $0.02 \text{ yr}^{-1}$ . This value is close to the estimate by Engelbracht et al. (1998) of  $0.03 \text{ yr}^{-1}$ , but considerably lower than the  $0.08 \text{ yr}^{-1}$  as estimated by Van Buren & Greenhouse (1994). In the following we assume that all pulsars that are left behind by SN type-II explosions form a PWN and evolve as discussed in Section 2. A key parameter for estimating the flux from these systems is the typical birth period  $P_0$  of pulsars, as the energy available for particle acceleration is  $\propto P_0^{-2}$ . Birth periods have been estimated for only a small number of objects, for example for the Crab pulsar where  $P_0 \approx 16$  ms. However, a relatively recent study based on the population of radio pulsars suggests a mean birth period of  $\langle P_0 \rangle \simeq 300$  ms, with a spread of  $\sigma_{P_0} \simeq 150$  ms (Faucher-Giguère & Kaspi 2006). More recently, a model taking into account the population of  $\gamma$ -ray pulsars as detected by the Fermi-LAT suggests a revision of the mean pulsar birth period down to  $\langle P_0 \rangle \simeq 50$  ms (Watters & Romani 2011). The Crab may therefore represent a rather extreme case. In the following we assume a fixed value of  $P_0 = 35$  ms and discuss the implications of this choice below. A conversion efficiency  $\epsilon = 0.5$  is chosen as discussed above. The

<sup>1</sup> Note that Atayan & Aharonian (1996) derive a factor of 2.24 for the case of a spherical emission region.

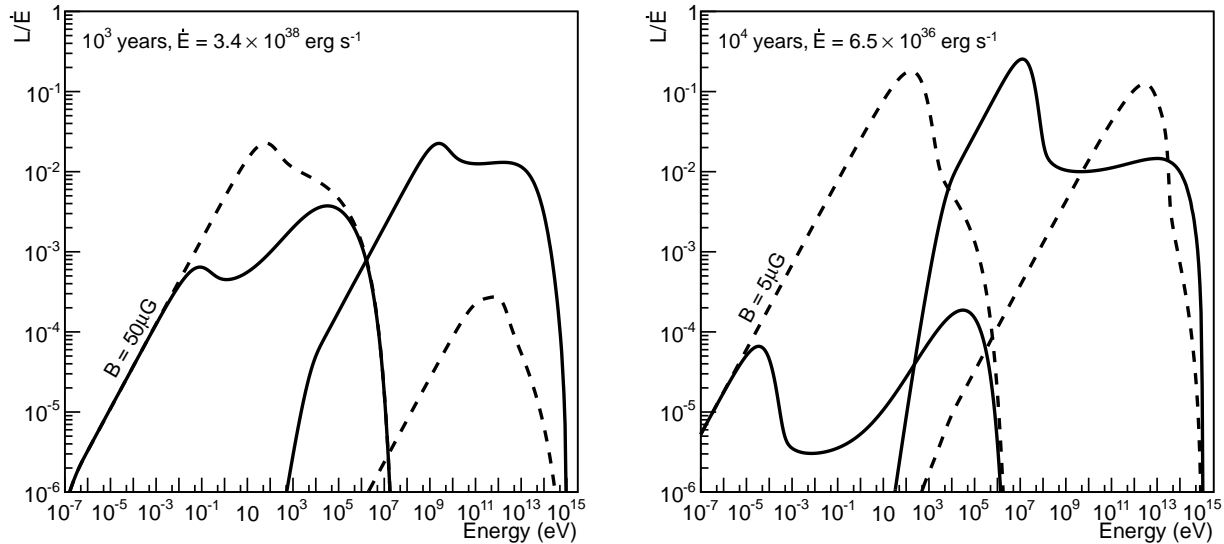


**Figure 1.** Fraction of the total power injected in electrons that is radiated in different spectral bands for a PWN with a “Crab-like” birth period of  $P_0 = 20$  ms and a braking index  $n = 3$ , after  $10^3$  yrs (left) and  $10^4$  yrs (right). The PWN is modeled as evolving in a SB-like (solid line) and ISM-like environment (dashed line), with a constant magnetic field strength of  $50\mu\text{G}$  (left) and  $5\mu\text{G}$  (right). The ISM radiation fields considered are, the CMB, a cold dust component with  $T = 50$  K and a starlight component with  $T = 5000$  K. Both radiation fields are assumed to have  $U_{\text{ph}} = 1$  eV  $\text{cm}^{-3}$ . The SB radiation field has a temperature of  $T = 50$  K and  $U_{\text{ph}} = 2400$  eV  $\text{cm}^{-3}$ . Note the difference in current spin-down power  $\dot{E}$  of a factor of  $\sim 50$  between  $10^3$  yrs and  $10^4$  yrs. The dominance of IC emission in the SB environment at all times is clearly visible.

magnetic field in a PWN is expected to decrease with time, however, in the SB environment energy losses are likely dominated by IC emission at all times and the  $B$ -field evolution is not expected to result in a modified particle energy distribution. We therefore assume no magnetic field evolution in the nebulae and use a mean  $B_{\text{PWN}}$  field value of  $25\mu\text{G}$ . As in the previous section we assume  $n = 3$ , and injection of particles with power-law index  $\alpha = 2.0$ .

The left-hand panel of Figure 2 shows a model spectral energy distribution (SED) for the total non-thermal emission of a population of PWNe in NGC 253’s SB at different evolutionary stages. This calculation is a two-zone, time-dependent model, where particles are injected in each PWN according to Equation 1. The number of PWN of a given age is calculated in 0.25 dex steps under the assumption of a constant pulsar birth rate as given above. Injected particles cool via IC and synchrotron processes in the PWN environment. For objects older than  $5 \times 10^4$  years, we assume that no more injection of particles in the PWN occurs, that all particles escape and continue to cool in the SB region of NGC 253. Non-thermal emission generated by this population of escaped particles add to the *diffuse* emission of NGC 253’s SB region. As the SB nucleus is characterised by a much higher magnetic field and average density ( $B_{\text{SB}} \simeq 250\mu\text{G}$ ,  $n_H \simeq 250\text{cm}^{-3}$ ) synchrotron, Bremsstrahlung and Coulomb losses become important for particles that have escaped the PWNe. The high thermal and cosmic-ray pressure in the SB region leads to the formation of a SB wind which effectively removes material from the centre of the galaxy. The height of the SB region of  $H \simeq 60$  pc and the wind speed of  $v_{\text{wind}} \simeq 300\text{km s}^{-1}$  (Zirakashvili & Völk 2006) implies an advective loss time of  $\tau_{\text{ad}} = (H/2)/v_{\text{wind}} \simeq 10^5$  yrs, after which particles are removed from the SB region. Hence, the SED for an age of  $1.5 \times 10^5$  yrs may well be representative of the equilibrium spectrum produced by all PWNe over the past 150 kyr. The SED for an age of  $5 \times 10^4$  yrs, on the other hand, shows the contribution of non-thermal particles that have not yet escaped their PWNe.

This SED therefore represents the contribution of *individual* PWN emission (rather than diffuse emission) to the overall non-thermal emission from the SB nucleus of NGC 253.

The right-hand panel of Figure 2 illustrates how the different energy-loss mechanisms shape the resulting SEDs. In the employed model, IC emission dominates at photon energies above  $\sim 100$  keV due to efficient cooling of non-thermal particles in the strong omnipresent FIR radiation field. The peak at  $\sim 500$  GeV in the  $\gamma$ -ray spectrum is caused by particles that have left their low-density PWNe environments after  $5 \times 10^4$  yrs and emit Bremsstrahlung in the dense gas of the SB region. The synchrotron emission spectrum is complex with a double-hump structure. Since the magnetic field in the SB region is so high, electrons with an energy of  $\gtrsim 1$  GeV that have left the PWNe predominantly lose energy via the synchrotron process and contribute to the radio emission. The second hump of the synchrotron spectrum in the X-ray domain is caused by the population of higher-energy particles that cool in the magnetic field of young PWNe. This figure also compares the two-zone model described above to a simple one-zone model. In this approach, particles are injected continuously rather than according to Equation 1, representing the semi-continuous nature of particle injection from the population of PWN as a whole. The environment in which particles cool in this calculation has been chosen to match the PWN environment for the target fields for processes that are important for the highest energy particles ( $B \simeq 25\mu\text{G}$  and SB radiation field), but using the mean SB density ( $n_H \simeq 250\text{cm}^{-3}$ ) for the calculation of Bremsstrahlung, as particles are expected to escape their PWN on roughly the Bremsstrahlung cooling time in the SB. Although the IC and Bremsstrahlung parts of the  $\gamma$ -ray spectra are quite similar, the synchrotron components look very different. This is a direct consequence of the two-zone model, with the low (high) magnetic field strengths inside (outside) of PWNe.

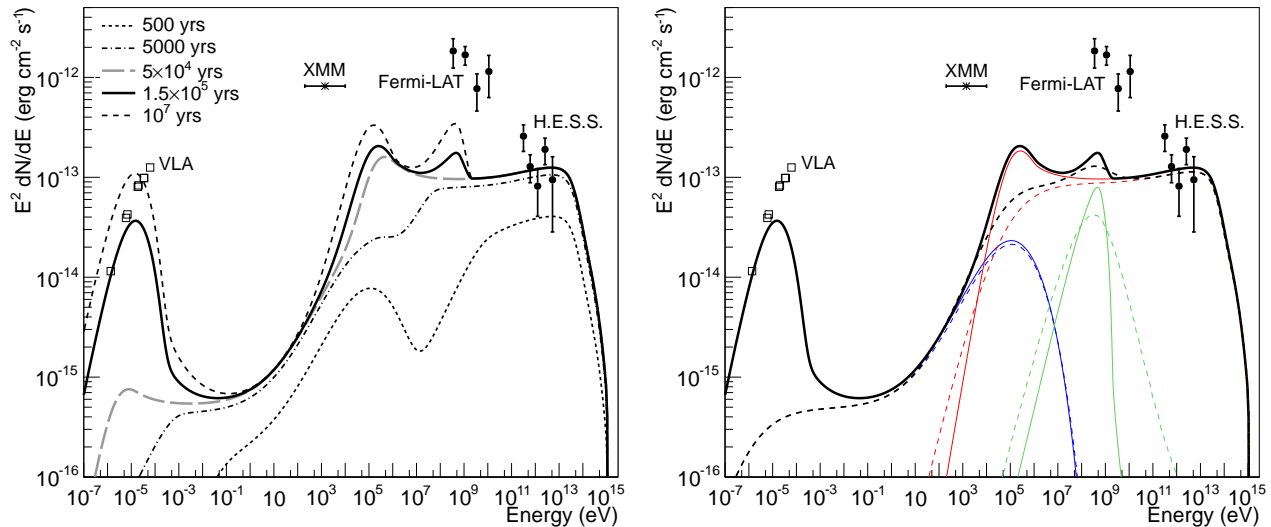


**Figure 2.** Predicted SEDs for PWNe populations in the SB environment of NGC 253 at different evolutionary stages. Also shown is radio data from the Very Large Array (VLA, Carilli 1996), the X-ray point is emission from the central source X 34 as given by Pietsch et al. (2001) and the Fermi-LAT and H.E.S.S. data is from Abramowski et al. (2012). *Left:* The integrated emission from *individual* PWNe is indicated by the long-dashed, grey curve. The equilibrium spectrum for all objects with ages less than  $1.5 \times 10^5$  yrs is given by the solid black curve. The effect of particle confinement in the SB region over the age of the SB episode of  $10^7$  yrs is indicated by the short-dashed black curve. *Right:* Equilibrium spectrum of NGC 253 for the two-zone, time-dependent model (straight lines) and for the simple one-zone model (dashed lines), both of which are described in the main text. The different components of the emission are IC (red), Bremsstrahlung (green) and synchrotron (blue).

### 3.2 M 82

In the following we apply the same two-zone model calculation to M 82 and compare it to multi-wavelength data from radio to VHE. The FIR emission from M 82's SB nucleus can be well described by a dominant dust component with a temperature of  $\sim 50$  K and a luminosity of  $3.8 \times 10^{10} L_{\odot}$  (Colbert et al. 1999). The inferred SFR is  $\sim 10 M_{\odot} \text{ yr}^{-1}$ , considerably higher than in NGC 253, and implies a type-II SN rate of  $\sim 0.06 \text{ yr}^{-1}$ . Adopting the disc-like SB geometry of 150 pc radius and 60 pc height as used in Strickland & Stevens (2000), the higher intensity of the FIR radiation in M 82's SB region also leads to a higher radiation field energy density of  $U_{\text{ph,M82}} \simeq 5000 \text{ eV cm}^{-3}$ . The magnetic field adopted here is the same as in NGC 253's SB:  $B_{\text{SB}} = 250 \mu\text{G}$ , consistent with estimates of  $200 \mu\text{G} - 400 \mu\text{G}$  (Thompson et al. 2006; Strickland & Heckman 2007). For the average density we again assume a value of  $n_H \simeq 250 \text{ cm}^{-3}$ .

Figure 3 shows the result for the two-zone model as described above. Particles are injected according to Equation 1 and for the estimated SN rate of  $0.06 \text{ yr}^{-1}$ . In order not to overproduce the emission measured by VERITAS, the pulsar birth period has been reduced to 40 ms. All other pulsar-related parameters are kept as above. As before the time after which particles leave the PWNe into the surrounding SB environment is fixed to  $5 \times 10^4$  years. Particles are again assumed to leave the SB region via energy-independent transport in the SB wind after  $1.5 \times 10^5$  yrs. The calculated SEDs have very similar shape to the curves obtained for NGC 253, as expected due to the similar target radiation field, magnetic fields, and average particle densities in the SB regions.

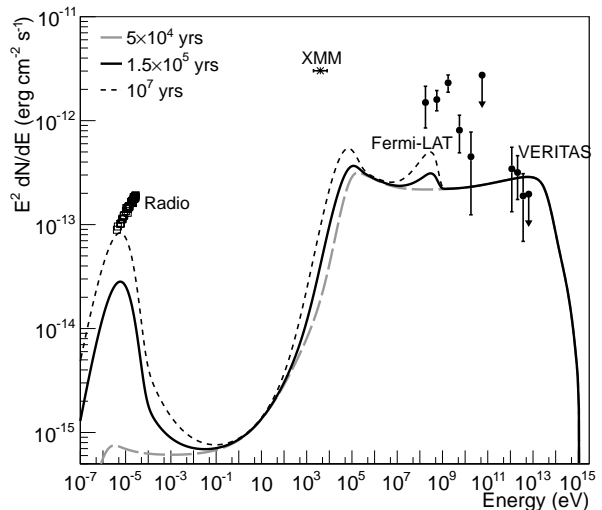


**Figure 3.** As Figure 2, but for the emission from PWNe that evolve in the SB environment of M 82. Multi-wavelength data is from Colbert et al. (1999, radio), Strickland & Heckman (2007, X-ray), Ackermann et al. (2012, HE  $\gamma$  rays) and VERITAS Collaboration (2009, VHE  $\gamma$  rays).

## 4 DISCUSSION

Figures 2 and 3 show that with a suitable choice of model parameters the VHE  $\gamma$ -ray emission of NGC 253 and M 82 may be dominated by PWN as suggested by Mannheim et al. (2012). In the following we discuss the plausibility of these parameter values.

**Magnetic and radiation fields.** Figure 2 shows that young PWNe are expected to dominate the HE and VHE  $\gamma$ -ray emission. Magnetic field strengths in young objects such as the Crab Nebula are estimated to be  $\sim 100 - 400 \mu\text{G}$  (Atoyan & Aharonian 1996;

Zhang et al. 2008; Volpi et al. 2008; Tanaka & Takahara 2010). The precise strengths of magnetic fields in these systems has little effect on the VHE fluxes unless the magnetic energy density  $U_B$  exceeds  $U_{\text{ph}}$ . Note PWNe that dominate in the Mannheim et al. (2012) model have much lower magnetic fields (de Jager et al. 2009). Our SB energy density estimates are based on a simplified geometry but are relatively robust, and exceed  $U_B$  as long as  $B < 500 \mu\text{G}$  (or even higher for M82). IC dominance over (at least most of) the early lifetime of pulsars in the SBs therefore seems likely.

**Particle Escape.** In our model we assume that all particles escape the PWNe after  $5 \times 10^4$  yrs. Smaller values of the escape time, and energy-dependent escape are certainly plausible (see e.g. Hinton et al. 2011) but have modest impact on the resulting SED except to boost diffuse synchrotron emission at high radio frequencies and bremsstrahlung emission at  $\sim 1$  GeV. The escape time of particles from the SB region must be less than  $\sim 1$  Myr to avoid violating constraints on the diffuse radio emission. However, energy independent escape via the SB wind on much shorter timescales seems likely (Zirakashvili & Völk 2006). For even higher wind speeds (e.g. Strickland & Heckman 2009), particles would escape the SB region faster and the Bremsstrahlung and radio components would be lower.

**Birth Period.** Average values of  $P_0$  (or strictly  $\langle P_0^2 \rangle^{1/2}$ ) of  $\sim 35$  ms and  $\sim 40$  ms are required to match the VHE fluxes of NGC 253 and M82, respectively. Whilst these values are somewhat lower than typical assumptions for pulsar populations, it is certainly possible that these values are representative of recently formed pulsars in these objects. Furthermore, a plausible increase of the injection efficiency  $\epsilon$  and/or a systematic underestimate in the SN rate, would increase these values into a more comfortable range.

**Injection spectrum.** The assumed hard injection spectrum ( $\alpha = 2$ ) maximises the VHE flux. Softer spectra at injection are plausible, and would be consistent with the measured VHE spectra, but increase the required energy input dramatically. For example for  $\alpha = 2.3$  the required birth periods are  $\sim 15$  ms and fast particle escape ( $t_{\text{esc}} \ll 10^5$  years) is required for consistency with radio limits. As a consequence PWN cannot explain the emission detected with Fermi from these objects.

## 5 CONCLUSIONS AND OUTLOOK

Considering the very different evolution of particle populations in starburst environments to typical Galactic environments we nevertheless reach a similar conclusion to that of Mannheim et al. (2012): that PWN can plausibly contribute to the TeV emission of NGC 253 and M82. The Fermi emission cannot be explained in this framework on energetics grounds and the standard explanation of diffuse emission from strong interactions of accelerated cosmic rays remains the most likely possibility. As a cut-off in this component just before the TeV range seems unlikely, the observed VHE emission may represent a superposition of a harder PWN component on the diffuse p-p emission. CTA (Actis et al. 2011) will have the sensitivity to search for the spectral feature associated with PWN and place tight constraints on the pulsar population.

## ACKNOWLEDGEMENTS

S.O. acknowledges the support of the Humboldt foundation by a Feodor-Lynen research fellowship.

## REFERENCES

- Abdo A. A. et al., 2010, ApJ, 709, L152  
 Abramowski A. et al., 2012, ApJ, 757, 158  
 Acero F. et al., 2009, Science, 326, 1080  
 Ackermann M. et al., 2012, ApJ, 755, 164  
 Actis M. et al., 2011, Experimental Astronomy, 32, 193  
 Akyuz A., Brouillet N., Ozel M. E., 1991, A&A, 248, 419  
 Atoyan A. M., Aharonian F. A., 1996, MNRAS, 278, 525  
 Carilli C. L., 1996, A&A, 305, 402  
 Colbert J. W. et al., 1999, ApJ, 511, 721  
 de Jager O. C., Djannati-Ataï A., 2009, in Astrophysics and Space Science Library, Vol. 357, Astrophysics and Space Science Library, Becker W., ed., p. 451  
 de Jager O. C. et al., 2009, ArXiv e-prints  
 Del Zanna L., Volpi D., Amato E., Bucciantini N., 2006, A&A, 453, 621  
 Engelbracht C. W., Rieke M. J., Rieke G. H., Kelly D. M., Achtermann J. M., 1998, ApJ, 505, 639  
 Faucher-Giguère C.-A., Kaspi V. M., 2006, ApJ, 643, 332  
 Gaensler B. M., Slane P. O., 2006, ARA&A, 44, 17  
 Gelfand J. D., Slane P. O., Zhang W., 2009, ApJ, 703, 2051  
 Hinton J. A., Aharonian F. A., 2007, ApJ, 657, 302  
 Hinton J. A., Funk S., Parsons R. D., Ohm S., 2011, ApJ, 743, L7  
 Hinton J. A., Hofmann W., 2009, ARA&A, 47, 523  
 Kennel C. F., Coroniti F. V., 1984, ApJ, 283, 694  
 Lacki B. C., Thompson T. A., Quataert E., Loeb A., Waxman E., 2011, ApJ, 734, 107  
 Mannheim K., Elsässer D., Tibolla O., 2012, Astroparticle Physics, 35, 797  
 Melo V. P., Pérez García A. M., Acosta-Pulido J. A., Muñoz-Tuñón C., Rodríguez Espinosa J. M., 2002, ApJ, 574, 709  
 Ohm S., Hinton J., 2012, in IAU Symposium, Vol. 284, IAU Symposium, pp. 382–388  
 Paglione T. A. D., Abrahams R. D., 2012, ApJ, 755, 106  
 Pietsch W. et al., 2001, A&A, 365, L174  
 Schöck F. M., Büsching I., de Jager O. C., Eger P., Vorster M. J., 2010, A&A, 515, A109  
 Slane P., Castro D., Funk S., Uchiyama Y., Lemiére A., Gelfand J. D., Lemoine-Goumard M., 2010, ApJ, 720, 266  
 Spitkovsky A., 2008, ApJ, 682, L5  
 Strickland D. K., Heckman T. M., 2007, ApJ, 658, 258  
 Strickland D. K., Heckman T. M., 2009, ApJ, 697, 2030  
 Strickland D. K., Stevens I. R., 2000, MNRAS, 314, 511  
 Tanaka S. J., Takahara F., 2010, ApJ, 715, 1248  
 Thompson T. A., Quataert E., Waxman E., Murray N., Martin C. L., 2006, ApJ, 645, 186  
 Van Buren D., Greenhouse M. A., 1994, ApJ, 431, 640  
 VERITAS Collaboration, 2009, Nature, 462, 770  
 Völk H. J., Klein U., Wielebinski R., 1989, A&A, 213, L12  
 Volpi D., Del Zanna L., Amato E., Bucciantini N., 2008, A&A, 485, 337  
 Watters K. P., Romani R. W., 2011, ApJ, 727, 123  
 Weaver K. A., Heckman T. M., Strickland D. K., Dahlem M., 2002, ApJ, 576, L19  
 Zhang L., Chen S. B., Fang J., 2008, ApJ, 676, 1210  
 Zirakashvili V. N., Völk H. J., 2006, ApJ, 636, 140